Journal of Medicinal Chemistry

Article

pubs.acs.org/jmc

Synthesis of New 4-Thiazolidinone-, Pyrazoline-, and Isatin-Based Conjugates with Promising Antitumor Activity

Dmytro Havrylyuk,[†] Borys Zimenkovsky,[†] Olexandr Vasylenko,[‡] Andrzej Gzella,[§,∥] and Roman Lesyk*[,†]

[†]Department of Pharmaceutical, Organic and Bioorganic Chemistry, Danylo Halytsky Lviv National Medical University, Pekarska 69, Lviv 79010, Ukraine

[‡]Institute of Bioorganic Chemistry and Petrochemistry, National Academy of Science of Ukraine, Murmanska 1, Kyiv 02094, Ukraine

[§]Department of Organic Chemistry, Poznan University of Medical Sciences, Grunwaldzka 6, Poznan 60780, Poland

[∥]Faculty of Pharmacy, Ludwik Rydygier Collegium Medicum in Bydgoszcz, Nicolaus Copernicus University in Toruń, M. Curie Skłodowskiej 9, Bydgoszcz 85094, Poland

Supporting Information

ABSTRACT: The synthesis and antitumor activity screening of novel 3-[2-(3,5-diaryl-4,5-dihydropyrazol-1-yl)-4-oxo-4,5-dihydro-1,3-thiazol-5-ylidene]-2,3-dihydro-1*H*-indol-2-ones **1**−**23** and 3-(3,5-diarylpyrazol-1-yl)-2,3-dihydro-1*H*-indol-2-ones **24**−**39** are performed. In vitro anticancer activity of the synthesized compounds was tested by the National Cancer Institute. Most of them displayed anticancer activity on leukemia, melanoma, lung, colon, CNS, ovarian, renal, prostate, and breast cancers cell lines. The structure−activity relationship is discussed. The most effective anticancer compound **10** was found to be active with mean GI_{50} and TGI values of 0.071 μM and 0.76 μM, respectively. It demonstrated the highest antiproliferative influence on the non-small-cell lung cancer cell line HOP-92 (GI_{50} < 0.01 μM), colon cancer line HCT-116 (GI_{50} = 0.018 μM), CNS cancer cell line SNB-75 (GI_{50} = 0.0159 μM), ovarian cancer cell line NCI/ADR-RES (GI_{50} = 0.0169 μM), and renal cancer cell line RXF 393 (GI_{50} = 0.0197 μM).

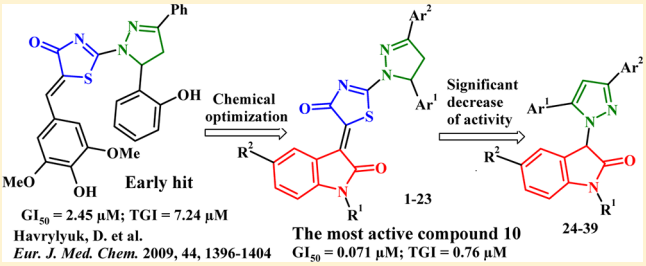

INTRODUCTION

The synthesis and biological activity evaluation of noncondensed systems containing thiazolidine,[1] pyrazoline,[2] and isatin[3] fragments are based upon previous results of experimental studies of these heterocycle derivatives as potential chemotherapeutic agents. Antitumor activity evaluation is actual and promising for these compounds (Figure 1). Antitumor mechanisms of 4-thiazolidinones can be associated with their affinity for JNK-stimulating phosphatase-1 (JSP-1),[4] tumor necrosis factor TNFα,[5] anti-apoptotic biocomplex Bcl-X_L-BH3,[6] integrin $\alpha_v\beta_3$ receptor,[7] nonmembrane protein tyrosine phosphatase (SHP-2),[8] etc. In addition, 1*H*-indole-2,3-dione derivatives possess potent anticancer activity as tyrosine kinase inhibitors,[9] inhibitors of cyclin-dependent kinases (CDKs),[10] inhibitors of plasma membrane electron transport,[11] and carbonic anhydrase isozyme inhibitors (CAIs).[12] On the other hand, various pyrazole and pyrazoline derivatives have been identified as inhibitors of cyclin-dependent kinase,[13] heat shock proteins,[14] vascular endothelium growth factors,[15] and P-glycoprotein.[16]

A pharmacophore hybrid approach for exploration of novel and highly active compounds is an effective and commonly used direction in modern medicinal chemistry. Hybridization of two different bioactive molecules with complementary pharmacophoric functions or with different mechanisms of action often showed synergistic effects.[17] This hypothesis was confirmed by the results of our previous studies that allowed identification of the high antitumor activity of 4-thiazolidinone derivatives coupled with other heterocyclic fragments in one molecule.[18]

In continuation of this theme, we designed (Figure 2) and synthesized new noncondensed heterocyclic compounds containing 4-thiazolidinone, 2,3-dihydro-1*H*-indol-2-one, and pharmacologically attractive pyrazole or pyrazoline moieties. The evaluation of their antitumor activity was carried out in vitro and in vivo. Combination of pyrazoline, 4-thiazolidinone, and 2,3-dihydro-1*H*-indol-2-one moieties in one molecule allowed gain of one or two logs of antitumor cytotoxicity at the GI_{50} level (−5.5 to −7.5, activity range) in comparison with pyrazole−indoline-2-one conjugates (−4.8 to −5.5) or pyrazoline−thiazolidinone analogous compounds (−4.1 to −5.6), reported previously.[19]

RESULTS AND DISCUSSION

Chemistry. The general methods for synthesis of target pyrazoline−thiazolidinone−isatin conjugates and pyrazole−indol-2-one analogs are depicted in Schemes 1 and 2.

3-[2-(3,5-Diaryl-4,5-dihydropyrazol-1-yl)-4-oxo-4,5-dihydro-1,3-thiazol-5-ylidene]-2,3-dihydro-1*H*-indol-2-ones **1**−**23** were

Received: June 6, 2012
Published: September 20, 2012

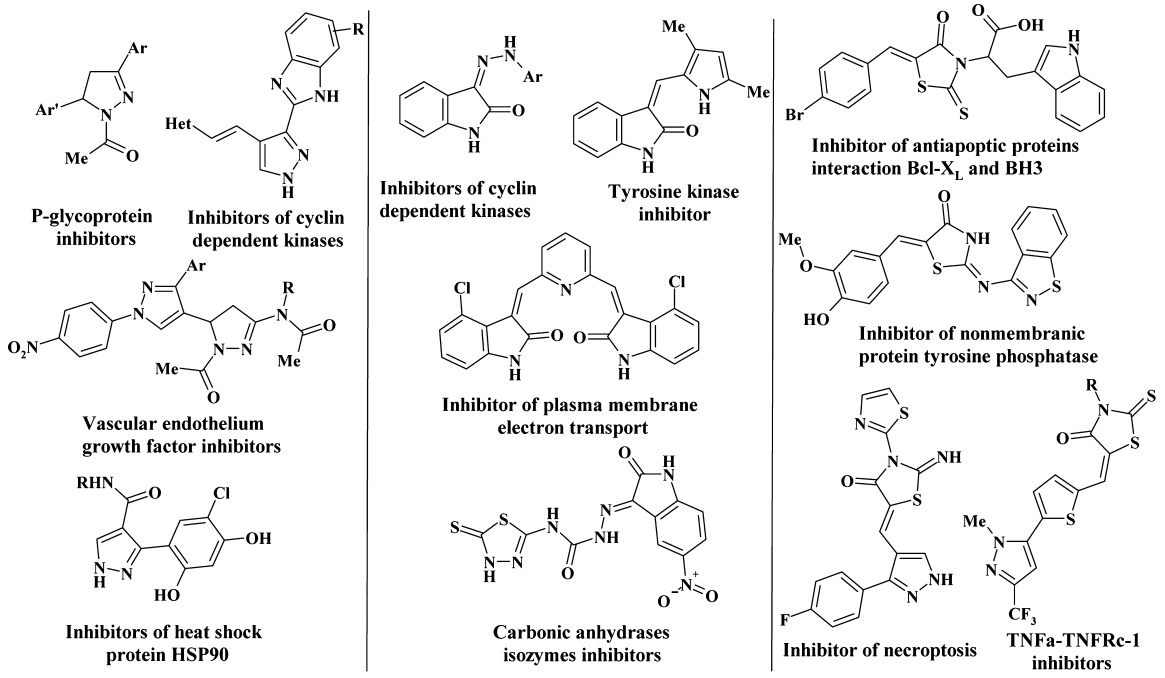

Figure 1. Structures of anticancer diazole, isatin, and 4-thiazolidinone derivatives.

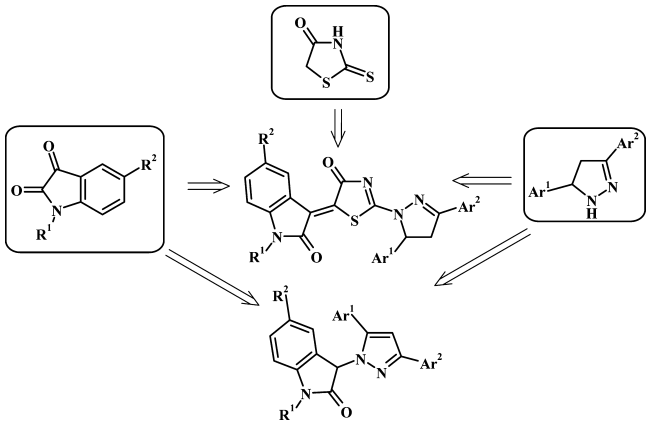

Figure 2. Design of the new noncondensed heterocyclic compounds with 4-thiazolidinone, 2,3-dihydro-1*H*-indol-2-one, and pyrazole or pyrazoline moieties.

synthesized via one-pot methodology involving reaction of 3,5-diaryl-1-thiocarbamoyl-2-pyrazolines with chloroacetic acid and appropriate isatins in the presence of fused sodium acetate in refluxing acetic acid (Scheme 1). Preparation of compound **3** as well as structures of the compounds **4** and **11** were described in our previous reports.[20]

It is known that the reaction of secondary amines with isatins passes through the formation of 3-dialkylamino-3-hydroxy-2,3-dihydro-1*H*-indol-2-ones and further indole cycle opening.[21] However, according to other published data, the reaction of isatin derivatives with 5-(2-hydroxyphenyl)-3-phenylpyrazoline yielded a spirosystem with 2-oxoindole and benzoxazinopyrazoline fragments.[22] Considering this ambiguous information, reaction features were studied between 3,5-diaryl-4,5-dihydro-1*H*-pyrazoles and isatins, and the structures of obtained products were identified. The above-mentioned reaction yielded the 3-(3,5-diarylpyrazol-1-yl)-2,3-dihydro-1*H*-indol-2-ones **24**−**39** (Scheme 2), which is not consistent with previously published data.[21,22]

The first stage of the reaction potentially follows a classic mechanism of a nucleophilic attack of the secondary amine in position C3 on isatin through the formation of 3-(3,5-diaryl-4,5-dihydropyrazol-1-yl)-3-hydroxy-2,3-dihydro-1*H*-indol-2-ones[21] followed by intramolecular redox reaction with dehydrogenation of pyrazoline cycle (Scheme 3).[23]

The analytical and spectral data (^{1}H NMR, ^{13}C NMR, LCMS) confirmed the structure and purity of **1**−**39**. ^{1}H NMR spectra of **1**−**23** show characteristic patterns of an AMX system for CH_2−CH protons of pyrazoline fragment. The chemical shifts of the protons H_A, H_M, and H_X have been assigned to $\delta \approx 3.41-3.66$, $\delta \approx 4.10-4.26$, and $\delta \approx 5.82-6.05$ with corresponding coupling constants of $J_{AM} = 17.5-18.7$, $J_{AX} = 10.4-11.3$, and $J_{MX} = 2.3-4.1$ Hz, respectively. The CH-group proton of 2,3-dihydro-1*H*-indol-2-one fragment in the ^{1}H NMR spectra of **24**−**39** appears as singlet at $\delta \approx 6.78-7.18$ ppm, and the CH proton of the pyrazole cycle has a singlet at $\delta \approx 5.79-6.21$.

Structural features of synthesized 3-[2-(3,5-diaryl-4,5-dihydropyrazol-1-yl)-4-oxo-4,5-dihydro-1,3-thiazol-5-ylidene]-2,3-dihydro-1*H*-indol-2-ones and 3-(3,5-diarylpyrazol-1-yl)-2,3-dihydro-1*H*-indol-2-ones were confirmed by X-ray crystallographic analysis of **23** (confirmed the structure of 1-methyl-3-[4-oxo-2-(3-phenyl-5-thiophen-2-yl-4,5-dihydropyrazol-1-yl)-4*H*-thiazol-5-ylidene]-2,3-dihydro-1*H*-indol-2-one) and **24** (confirmed the structure of {3-[5-(2-hydroxyphenyl)-3-phenylpyrazol-1-yl]-2-oxo-2,3-dihydroindol-1-yl}-acetic acid ethanol disolvate).

The geometry of **23** is shown at Figure 3, and its structure can be represented by the mesomeric structures **A** and **B** in which the C2 atom of 1,3-thiazol-4-one system is connected to the endo- (N3) or exocyclic (N6) nitrogen atom via a double bond (Figure 4).

In the crystal lattice, the molecules take up a structure intermediate (form **C**) between structures **A** and **B** (Figure 4). This conclusion was drawn on the basis of similar values of the interatomic distances for C2−N3 [1. 1.300(3) Å] and C2−N6

dx.doi.org/10.1021/jm300789g | J. Med. Chem. 2012, 55, 8630−8641

Scheme 1. Synthesis of 3-[2-(3,5-Diaryl-4,5-dihydropyrazol-1-yl)-4-oxo-4,5-dihydro-1,3-thiazol-5-ylidene]-2,3-dihydro-1*H*-indol-2-ones[a]

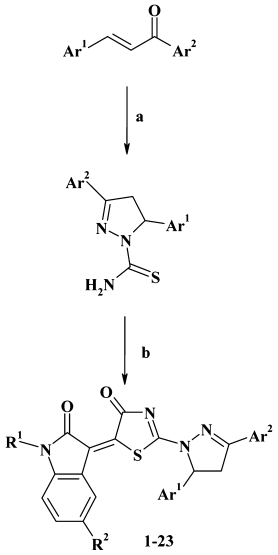

Comp	Ar^1	Ar^2	R^1	R^2
1	2-OH-C_6H_4	Ph	H	H
2	2-OH-C_6H_4	Ph	H	Br
3	4-OMe-C_6H_4	Ph	H	H
4	4-OMe-C_6H_4	Ph	H	Br
5	4-OMe-C_6H_4	Ph	CH_2COOH	H
6	4-OMe-C_6H_4	4-OMe-C_6H_4	H	H
7	4-OMe-C_6H_4	4-OMe-C_6H_4	H	Br
8	4-OMe-C_6H_4	4-OMe-C_6H_4	H	Cl
9	4-OMe-C_6H_4	naphthalen-2-yl	H	H
10	4-OMe-C_6H_4	naphthalen-2-yl	H	Br
11	4-Cl-C_6H_4	Ph	H	H
12	4-Cl-C_6H_4	Ph	H	Me
13	4-Cl-C_6H_4	4-OMe-C_6H_4	H	H
14	4-Cl-C_6H_4	4-OMe-C_6H_4	H	Br
15	4-Cl-C_6H_4	4-OMe-C_6H_4	H	Cl
16	4-Cl-C_6H_4	4-OMe-C_6H_4	Me	H
17	4-Cl-C_6H_4	naphthalen-2-yl	H	H
18	4-NMe_2-C_6H_4	Ph	H	H
19	4-NMe_2-C_6H_4	Ph	H	Br
20	4-NMe_2-C_6H_4	Ph	H	Cl
21	thiophen-2-yl	Ph	H	H
22	thiophen-2-yl	Ph	H	Br
23	thiophen-2-yl	Ph	Me	H

[a]Reagents, conditions, and yields: (a) thiosemicarbazide (1.2 equiv), KOH (2.5 equiv), EtOH, reflux 8 h (ref 30); (b) appropriate isatin (1.2 equiv), $ClCH_2COOH$ (1.0 equiv), AcONa (2.0 equiv), AcOH, reflux 5 h, 62−85%.

Scheme 2. Synthesis of 3-[3,5-Diarylpyrazol-1-yl]-2,3-dihydro-1*H*-indol-2-ones[a]

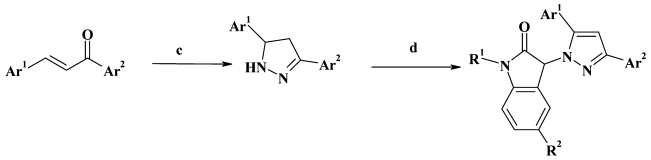

Comp	Ar^1	Ar^2	R^1	R^2
24	2-OH-C_6H_4	Ph	CH_2COOH	H
25	4-OMe-C_6H_4	4-OMe-C_6H_4	H	H
26	4-OMe-C_6H_4	4-OMe-C_6H_4	H	Br
27	4-OMe-C_6H_4	4-OMe-C_6H_4	H	Cl
28	4-Cl-C_6H_4	Ph	H	H
29	4-Cl-C_6H_4	Ph	H	Br
30	4-Cl-C_6H_4	Ph	CH_2COOH	H
31	4-Cl-C_6H_4	4-OMe-C_6H_4	H	H
32	4-Cl-C_6H_4	4-OMe-C_6H_4	H	Br
33	4-Cl-C_6H_4	4-OMe-C_6H_4	H	Cl
34	4-NMe_2-C_6H_4	Ph	H	H
35	4-OMe-C_6H_4	naphthalen-2-yl	H	H
36	4-OMe-C_6H_4	naphthalen-2-yl	H	Cl
37	4-Cl-C_6H_4	naphthalen-2-yl	H	H
38	4-Cl-C_6H_4	naphthalen-2-yl	H	Br
39	4-Cl-C_6H_4	naphthalen-2-yl	CH_2COOH	H

[a]Reagents, conditions, and yields: (c) hydrazine hydrate (1.0 equiv), EtOH, reflux 0.5 h (ref 29); (d) appropriate isatin (1.0 equiv), EtOH, reflux 1 h, 68−83%.

Scheme 3. Proposed Mechanism of 3-(3,5-Diarylpyrazol-1-yl)-2,3-dihydro-1*H*-indol-2-one Formation

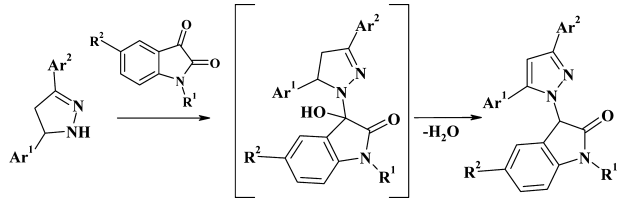

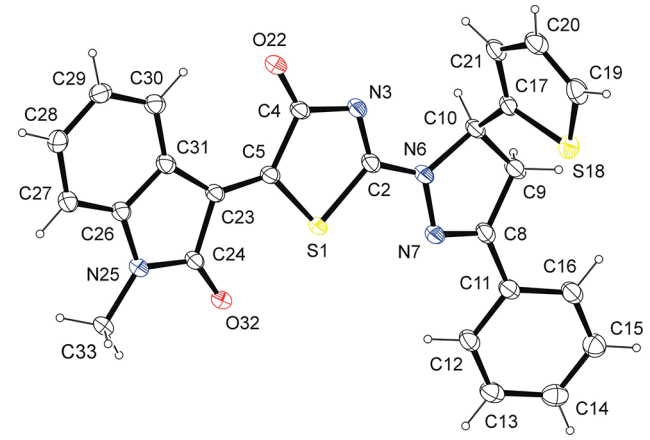

Figure 3. View of **23**. Displacement ellipsoids are drawn at the 30% probability level, and H atoms are depicted as spheres of arbitrary radii.

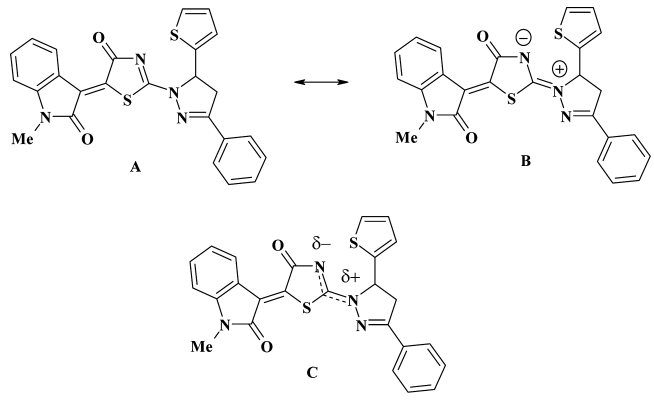

Figure 4. Two mesomeric structures (**A** and **B**) of **23** and the molecular structure (form **C**) found in the crystal.

[1.328(3) Å] indicating that these two bonds have a partial double-bond character in the molecules. The distances are longer

dx.doi.org/10.1021/jm300789g | J. Med. Chem. 2012, 55, 8630−8641

by 7 and 15σ, respectively, than a regular double bond length C=N [1.279(1) Å].[24]

In molecule **23**, only the 4,5-dihydropyrazole ring is slightly puckered (rms deviation 0.0382 Å) and has an envelope-oriented conformation [Cremer and Pople[25] puckering parameters: $Q(2)$ = 0.086(3) Å, $\varphi(2)$ = 318.2(18)°]. The four atoms N6, N7, C8, and C9 are coplanar [maximum deviation from the least-squares plane of 0.0049(14) Å], while the fifth atom C10 is out of this plane [0.141(4) Å].

The asymmetric unit of **24** contains one solute molecule (host) and two solvent (ethanol) molecules (guests) (Figure 5).

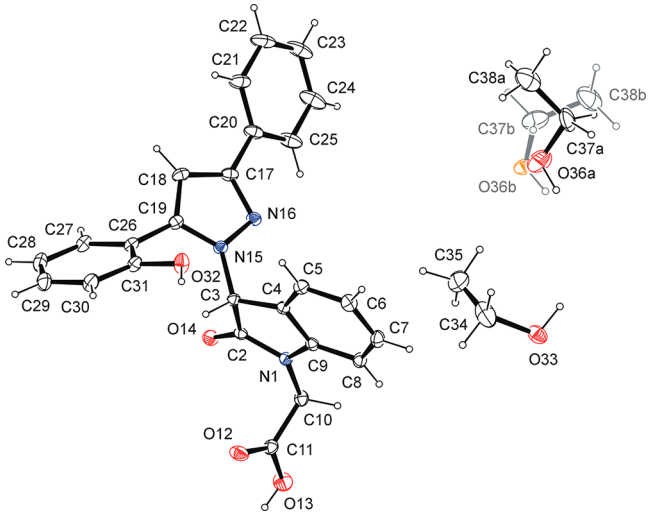

Figure 5. View of **24**. Displacement ellipsoids are drawn at the 30% probability level, and H atoms are depicted as spheres of arbitrary radii.

The architecture of the crystal structure of **24** is determined mainly by O–H···O hydrogen bonds involving ethanol molecules, which act both as a donor and an acceptor.

Evaluation of Anticancer Activity in Vitro and in Vivo. Synthesized 3-[2-(3,5-diaryl-4,5-dihydropyrazol-1-yl)-4-oxo-4,5-dihydro-1,3-thiazol-5-ylidene]-2,3-dihydro-1*H*-indol-2-ones (**1**–**20**) and 3-(3,5-diarylpyrazol-1-yl)-2,3-dihydro-1*H*-indol-2-ones (**24**–**39**) were submitted and evaluated at the single concentration of 10 μM toward a panel of approximately 60 cancer cell lines. The human tumor cell lines were derived from nine different cancer types: leukemia, melanoma, lung, colon, CNS, ovarian, renal, prostate, and breast cancers. Primary anticancer assays were performed according to the US NCI protocol (http://dtp.nci.nih.gov), as described elsewhere.[26] The compounds were added at the single concentration, and the cell culture was incubated for 48 h. The end point determinations were made with a protein binding dye, sulforhodamine B (SRB). The results for each compound are reported as the growth percentage (GP%) of treated cells compared with untreated control cells (Table 1). A range of growth % shows the lowest and the highest growth % found among different cancer cell lines.

The synthesized pyrazoline–thiazolidinone–isatin conjugates **1**–**4**, **7**–**12**, **14**, **15**, and **17**–**20** displayed significant activity in the in vitro screen on tested cell lines in 10 μM concentration (Table 1). These compounds demonstrated a cytotoxic effect on the most of the tumor cell lines. One derivative of this group, **6**, showed moderate activity, and three compounds, **5**, **13**, and **16**, were inactive. The pyrazole derivatives with 2,3-dihydro-1*H*-indol-2-one fragment (**24**–**39**) were far less active than the noncondensed systems with three heterocycles (**1**–**20**), emphasizing the importance of presence and positioning of central linker between two terminal heterocycles, well represented by 4-thiazolidinone moiety, which is coplanar with the indolone part in the target compounds with potent antitumor properties. Only four compounds from this group, **32**–**34** and **38**, demonstrated moderate activity in 10 μM concentration (GP = 50.79–70.89%) with the selective influence on several leukemia (CCRF-CEM and HL-60) and ovarian cancer (OVCAR-4) cell lines.

Finally, compounds **1**–**4**, **6**–**15**, **17**–**20**, **32**–**34**, and **38** were selected in advanced assay against a panel of approximately 60 tumor cell lines at 10-fold dilutions of five concentrations (100, 10, 1, 0.1, and 0.01 μM).[26] Based on the cytotoxicity assays, three antitumor activity dose–response parameters were calculated for experimental agents against each cell line: GI_{50}, molar concentration of the compound that inhibits 50% net cell growth; TGI, molar concentration of the compound leading to total inhibition; LC_{50}, molar concentration of the compound leading to 50% net cell death. Furthermore a mean graph midpoints (MG_MID) were calculated for each of the parameters, giving an average activity parameter over all cell lines for the tested compounds. For the calculation of the MG_MID, insensitive cell lines are included with the highest concentration tested (Table 2). Some of the compounds were retested on the basis of the results of the first screen: compounds **4**, **7**–**12**, **14**, **15**, **17**, and **19** twice, compound **18** in triple, and all other compounds were tested once.

The above NCI screening data analysis indicated that most of members of the pyrazoline–thiazolidinone–isatin series (**1**–**4**, **7**–**12**, **14**, **15**, and **17**–**20**) possessed potent in vitro antiproliferative activity, with mean GI_{50} values across the 60 cell lines ranging from 0.071 (**10**) to 8.05 μM (**18**). Activities of **6** and **14** were insignificant. The pyrazole–indole conjugates **32**–**34**, and **38** were less active compared with their 4-thiazolidinone-containing analogues with mean GI_{50} values from 4.47 to 18.06 μM.

The most active compound in the series of pyrazoline–thiazolidinone–isatin conjugates is the 5-bromo-3-{2-[5-(4-methoxyphenyl)-3-naphthalen-2-yl-4,5-dihydropyrazol-1-yl]-4-oxo-4,5-dihydro-1,3-thiazol-5-ylidene}-2,3-dihydro-1*H*-indol-2-one **10**, both in terms of the mean GI_{50} (0.071 μM) and TGI (0.76 μM). Notably, this compound ranks as nearly 100-fold more potent (mean GI_{50}) compared with the most potent member of the 2-[3,5-diaryl-4,5-dihydropyrazol-1-yl]thiazol-4(5*H*)-ones, reported previously.[19] At the second assay (Table 3), the compound **10** was found to be a highly active growth inhibitor of the non-small-cell lung cancer cell line HOP-92 (GI_{50} < 0.01 μM), colon cancer line HCT-116 (GI_{50} = 0.018 μM), CNS cancer cell line SNB-75 (GI_{50} = 0.0159 μM), ovarian cancer cell line OVCAR-3 (GI_{50} = 0.0216 μM), and renal cancer cell line RXF 393 (GI_{50} = 0.0197 μM). Mean pGI_{50}, pTGI, and pLC_{50} of compound **10** in comparison with standard anticancer agent are given at Figure 6.

The SAR study revealed that (1) potent anticancer activity of tested compounds depended on the presence of a combination of three heterocycles in one molecule; thus the pyrazoline–thiazolidinone–isatin conjugates were more active in comparison with pyrazoline–thiazolidinone[19] or pyrazole–indoline-2-one systems; (2) attachment of halogen (Br or Cl) to 5-position of isatin scaffold (**2**, **4**, **7**, **8**, **10**, **14**, **15**, **19**, **20**, **32**, **33**, **38**) allowed us to gain of one log unit of activity (GI_{50} level), in comparison with 5-unsubstituted isatin analogs; (3) introduction of a methyl group or CH_2COOH group at 1*N*-position of isatin fragment (**5**,

dx.doi.org/10.1021/jm300789g | J. Med. Chem. 2012, 55, 8630–8641

Table 1. Anticancer Screening Data in Concentration 10.00 μM

	60 cell lines assay in one dose 10.00 μM concn				
compd	mean growth, %	range of growth, %	most sensitive cell lines	positive cytostatic effect[a]	positive cytotoxic effect[b]
1	−37.37	−77.15 to 16.01	HCT-116 (colon cancer)	4/53	49/53
2	−53.88	−98.23 to 7.54	SK-MEL-5 (melanoma)	3/58	55/58
3	−51.39	−94.59 to 19.90	OVCAR-3 (ovarian cancer)	7/60	53/60
4	−55.11	−95.64 to 7.87	SF-539 (CNS cancer)	4/60	56/60
5	97.34	37.46 to 183.90	TK-10 (renal cancer)	2/60	0/60
6	44.73	−69.94 to 117.74	U251 (CNS cancer)	21/54	7/54
7	23.86	−72.59 to 114.93	U251 (CNS cancer)	15/56	21/56
8	0.80	−84.01 to 109.79	NCI-H522 (NSC lung cancer)	18/57	30/57
9	−26.26	−90.18 to 54.01	U251 (CNS cancer)	13/57	41/57
10	−59.81	−100.00 to −1.59	SK-MEL-5 (melanoma)	0/59	59/59
11	−56.90	−100.00 to 35.68	SK-MEL-5 (melanoma)	3/53	50/53
12	−53.95	−100.00 to 88.69	U251 (CNS cancer)	3/57	53/57
13	77.45	−9.26 to 129.52	OVCAR-3 (ovarian cancer)	10/59	1/59
14	−56.40	−97.72 to 52.12	SK-MEL-5 (melanoma)	3/59	55/59
15	−58.01	−96.37 to 36.74	U251 (CNS cancer)	2/54	52/54
16	101.66	79.31 to 120.75	NCI-H522 (NSC lung cancer)	0/56	0/56
17	−25.09	−91.19 to 111.03	U251 (CNS cancer)	14/60	44/60
18	−39.61	−100.00 to 72.46	U251 (CNS cancer)	8/57	48/57
19	−51.12	−99.37 to 38.89	U251 (CNS cancer)	6/59	53/59
20	−52.88	−91.70 to 4.28	SK-MEL-5 (melanoma)	2/59	57/59
24	107.55	80.14 to 131.25	SNB-75 (CNS cancer)	0/58	0/58
25	87.55	35.22 to 130.24	NCI-H522 (NSC lung cancer)	1/58	0/58
26	88.62	5.70 to 108.98	NCI-H522 (NSC lung cancer)	1/56	0/56
27	82.02	6.53 to 113.49	NCI-H522 (NSC lung cancer)	3/58	0/58
28	76.57	−8.87 to 134.63	NCI-H522 (NSC lung cancer)	1/54	1/54
29	90.10	41.05 to 159.82	786-0 (renal cancer)	2/58	0/58
30	97.73	−64.97 to 123.59	CCRF-CEM (leukemia)	0/57	3/57
31	75.58	−63.11 to 107.51	CCRF-CEM (leukemia)	3/58	1/58
32	58.62	−61.05 to 112.65	CCRF-CEM (leukemia)	14/59	2/59
33	50.79	−43.02 to 101.17	CCRF-CEM (leukemia)	17/59	4/59
34	70.89	−52.14 to 122.45	HL-60 (TB) (leukemia)	8/57	3/57
35	91.46	53.09 to 121.07	OVCAR-4 (ovarian cancer)	0/58	0/58
36	98.23	77.23 to 115.51	MOLT-4 (leukemia)	0/58	0/58
37	90.83	2.70 to 122.50	NCI-H522 (NSC lung cancer)	8/58	0/58
38	58.49	−50.93 to 97.67	OVCAR-4 (ovarian cancer)	15/58	2/58
39	102.90	−7.58 to 127.27	CCRF-CEM (leukemia)	0/59	1/59

[a]Ratio between number of cell lines with percent growth from 0 to 50 and total number of cell lines. [b]Ratio between number of cell lines with percent growth of <0 and total number of cell lines.

16, **24**, **30**, **39**) led to the loss of activity; (4) the nature of a substituent in the 5-aryl fragment also had an influence on the antitumor activity. Therefore, the introduction of an electron-withdrawing group, −4-chlorine (**11**), improved the antiproliferative activity in comparison with electron-donor groups 2-OH (**1**), 4-OMe (**3**), and NMe_2 (**18**) groups. This would indicate that decreased of electron density on 5-aryl moiety is important for the inhibitory activity; and (5) substitution of the phenyl fragment in 3 position of pyrazoline cycle on naphthalene-2-yl substituent (compounds **9**, **10**, **17**, **35**−**37**, and **39**, except **38**) did not have significant influence on antitumor activity, but introduction of the 4-methoxyphenyl group in the mentioned position (**6**, **13**) limited this effect (Figure 7).

Nontumored Animal Toxicity Assays for **4**, **10**, **13**, **17**, and **18** were performed according to NCI protocol (http://dtp.nci.nih.gov/branches/btb/acute_tox.html). The results have shown that the maximum tolerated dose was more than 400 mg/kg. It can be used to calculate the amount of material to be given to experimental mice during further antitumor testing in vivo.

In Vivo Anticancer Activity: Hollow Fiber Assay. Compounds **4**, **10**, **13**, **17**, and **18**, which possessed promising activity during in vitro anticancer drug screening, were evaluated by NCI using the hollow fiber assay. This assay provided quantitative indications of the compound's drug efficacy (http://dtp.nci.nih.gov/branches/btb/hfa.html).[27] In a hollow fiber model, polyvinylidene fluoride fibers containing various human cancer cell cultures were implanted intraperitoneally (ip) and subcutaneously (sc) into athymic nude mice and compounds were administrated by the ip route. The effects of the compounds on reduction of the viable cancer cell mass compared to control were determined. To simplify evaluation, the NCI protocol adopts a point system that allows rapid viewing of the activity of a given compound. For this, a value of 2 is assigned for each compound dose that results in 50% or greater reduction in the viable cell mass. Compounds with a combined ip + sc score of ≥20, sc score of ≥8, or net cell kill of one or more cell lines were considered significantly active. The tested compounds did not show significant activity in the hollow fiber assay. Compound **4** resulted in an sc score of 2, compound **11** exhibited an sc score of

dx.doi.org/10.1021/jm300789g | J. Med. Chem. 2012, 55, 8630−8641

Table 2. Averaged Anticancer Activity (μM) against a Panel of Approximately 60 Tumor Cell Lines from Nine Different Cancer Types at 10-Fold Dilutions of Five Concentrations

compd	end point	leukemia	NSC lung cancer	colon cancer	CNS cancer	melanoma	ovarian cancer	renal cancer	prostate cancer	breast cancer	MG_MID
1	GI_{50} (μM)	3.19	2.03	1.99	2.13	2.04	2.41	2.07	2.05	2.09	2.22
	TGI (μM)	48.77	4.73	4.22	5.37	4.40	36.60	17.76	4.35	4.77	14.55
	LC_{50} (μM)	100.0	57.16	33.35	68.12	60.79	81.46	55.76	54.69	64.61	63.99
2	GI_{50} (μM)	0.27	0.24	0.21	0.24	0.23	0.28	0.23	0.29	0.26	0.25
	TGI (μM)	1.05	0.67	0.46	0.72	0.66	0.94	0.63	0.93	0.80	0.76
	LC_{50} (μM)	9.49	7.24	1.67	4.12	2.43	18.99	2.55	7.68	3.59	6.42
3	GI_{50} (μM)	1.64	2.38	1.81	1.62	2.00	2.30	2.01	1.52	2.02	1.92
	TGI (μM)	20.81	6.04	4.39	3.45	4.51	19.03	4.27	3.35	4.58	7.82
	LC_{50} (μM)	92.95	70.75	32.04	7.39	37.99	71.06	34.33	7.37	38.98	43.65
4[a]	GI_{50} (μM)	0.25	0.20	0.19	0.18	0.21	0.23	0.18	0.24	0.20	0.21
	TGI (μM)	4.23	0.51	0.39	0.39	0.55	3.63	0.36	0.66	0.48	1.24
	LC_{50} (μM)	51.02	3.275	1.07	6.48	5.01	23.42	1.27	39.47	26.54	17.51
6	GI_{50} (μM)	100.0	88.07	100.0	43.91	100.0	92.15	85.17	100.0	81.53	87.87
	TGI (μM)	100.0	91.55	100.0	89.15	100.0	100.0	100.0	100.0	99.58	97.80
	LC_{50} (μM)	100.0	100.0	100.0	100.0	100.0	100.0	100.0	100.0	100.0	100.0
7[a]	GI_{50} (μM)	0.28	0.20	0.20	0.20	0.19	0.24	0.20	0.27	0.21	0.22
	TGI (μM)	62.71	0.43	25.29	0.405	0.41	32.49	0.38	0.71	0.48	15.07
	LC_{50} (μM)	100.0	75.2	50.37	70.19	17.26	78.72	64.63	100.0	66.90	73.85
8[a]	GI_{50} (μM)	0.28	0.20	0.21	0.20	0.19	0.23	0.19	0.25	0.22	0.22
	TGI (μM)	75.15	0.44	0.43	0.42	0.38	21.20	0.39	0.71	0.50	11.91
	LC_{50} (μM)	100	64.22	58.72	35.49	33.87	83.45	50.47	100.0	75.19	66.82
9[a]	GI_{50} (μM)	17.50	0.62	1.68	0.67	4.80	0.97	0.87	0.36	5.96	3.16
	TGI (μM)	59.63	4.03	12.36	12.57	27.03	24.19	13.60	2.47	32.79	20.96
	LC_{50} (μM)	97.50	48.73	38.33	48.21	64.07	66.91	51.27	100.0	73.68	65.41
10[a]	GI_{50} (μM)	0.13	0.054	0.05	0.046	0.069	0.11	0.064	0.059	0.061	0.071
	TGI (μM)	3.37	0.22	0.14	0.21	0.19	0.85	0.33	0.51	0.99	0.76
	LC_{50} (μM)	87.76	41.53	1.15	3.42	3.52	18.81	5.19	13.81	2.65	19.76
11[a]	GI_{50} (μM)	0.37	0.23	0.19	0.19	0.28	0.23	0.27	0.25	0.32	0.26
	TGI (μM)	70.77	6.29	0.39	0.50	0.54	0.65	0.85	0.85	0.91	9.08
	LC_{50} (μM)	100.0	30.01	0.81	2.07	1.00	26.67	22.09	-	39.44	27.76
12[a]	GI_{50} (μM)	0.39	0.21	0.23	0.24	0.30	0.26	0.24	0.31	0.80	0.32
	TGI (μM)	39.39	0.62	0.35	0.32	0.67	-	0.52	-	100.0	15.74
	LC_{50} (μM)	85.17	100.0	100.0	75.22	100.0	100.0	100.0	100.0	100.0	95.53
13	GI_{50} (μM)	86.55	92.37	100.0	77.48	100.0	100.0	100.0	100.0	100.0	95.15
	TGI (μM)	90.86	100.0	100.0	100.0	100.0	100.0	100.0	100.0	100.0	98.98
	LC_{50} (μM)	100.0	100.0	100.0	100.0	100.0	100.0	100.0	100.0	100.0	100.0
14[a]	GI_{50} (μM)	0.19	0.12	0.13	0.12	0.16	0.19	0.14	0.18	0.14	0.15
	TGI (μM)	14.01	0.34	7.44	1.48	0.34	14.67	0.37	1.01	0.40	4.45
	LC_{50} (μM)	100.0	12.39	16.06	15.71	0.99	29.75	4.00	100.0	19.17	33.12
15[a]	GI_{50} (μM)	0.27	0.20	0.21	0.19	0.20	0.27	0.20	0.27	0.20	0.22
	TGI (μM)	0.89	0.46	0.45	0.43	0.44	7.97	0.46	0.74	0.47	1.37
	LC_{50} (μM)	91.13	7.93	8.20	12.67	1.21	31.34	13.75	76.23	25.74	29.80
17[a]	GI_{50} (μM)	19.14	0.46	0.53	8.80	0.35	15.37	0.40	0.40	0.74	5.13
	TGI (μM)	71.59	20.91	70.27	27.32	24.67	56.14	42.14	50.72	38.34	44.68
	LC_{50} (μM)	93.10	100.0	83.75	75.86	83.00	100.0	75.50	100.0	91.73	89.21
18[b]	GI_{50} (μM)	33.91	7.42	2.55	1.11	6.90	1.22	6.37	0.27	5.26	8.05
	TGI (μM)	45.62	25.2	35.30	3.24	29.42	39.71	18.84	34.02	20.25	27.96
	LC_{50} (μM)	94.83	48.95	40.36	41.61	43.90	47.12	43.02	41.37	57.30	50.94
19[a]	GI_{50} (μM)	0.31	0.22	0.20	0.21	0.20	0.25	0.20	0.27	0.22	0.23
	TGI (μM)	1.29	0.54	0.42	0.45	0.46	0.69	0.45	0.72	0.51	0.62
	LC_{50} (μM)	84.75	17.01	1.22	12.27	7.65	39.58	7.47	55.29	18.74	27.13
20	GI_{50} (μM)	0.34	0.21	0.19	0.19	0.26	0.24	0.19	0.25	0.22	0.23
	TGI (μM)	3.11	0.51	0.41	0.43	0.57	0.62	0.43	0.69	0.53	0.80
	LC_{50} (μM)	100.0	37.91	16.48	1.63	2.16	48.80	15.35	12.81	2.32	26.38
32	GI_{50} (μM)	12.35	7.53	7.20	5.48	13.22	9.75	9.20	7.65	8.10	8.94
	TGI (μM)	67.00	30.01	36.32	16.74	49.28	28.66	32.33	22.10	24.56	34.11
	LC_{50} (μM)	100.0	58.64	78.77	46.50	81.14	64.83	62.10	61.20	65.84	68.78
33	GI_{50} (μM)	27.95	4.37	6.15	3.94	9.40	3.68	3.75	6.49	6.29	8.00
	TGI (μM)	79.23	23.22	28.62	14.39	46.72	14.65	13.21	20.32	17.77	28.68

dx.doi.org/10.1021/jm300789g | J. Med. Chem. 2012, 55, 8630−8641

Table 2. continued

compd	end point	leukemia	NSC lung cancer	colon cancer	CNS cancer	melanoma	ovarian cancer	renal cancer	prostate cancer	breast cancer	MG_MID
	LC_{50} (μM)	100.0	59.78	69.40	42.20	76.41	52.26	42.43	62.40	47.64	61.39
34	GI_{50} (μM)	16.31	16.16	16.11	21.20	19.60	18.86	17.44	16.08	20.82	18.06
	TGI (μM)	74.58	56.01	39.72	68.65	54.52	67.24	57.30	74.05	73.36	62.82
	LC_{50} (μM)	100.0	90.88	79.05	95.08	91.25	93.32	86.21	100.0	90.14	91.77
38	GI_{50} (μM)	10.39	3.31	4.33	3.18	6.53	3.09	2.50	2.57	4.30	4.47
	TGI (μM)	15.17	10.04	15.00	10.51	22.36	9.85	7.66	8.89	14.30	14.86
	LC_{50} (μM)	79.21	34.45	51.08	33.27	56.84	33.20	27.21	34.35	62.08	45.74

[a]Compound was tested twice. [b]Compound was tested three times.

4, and compound **10** resulted in an ip score of 6, with low cytotoxic activity (no cell death).

COMPARE Analysis. The NCI's COMPARE algorithm (http://dtp.nci.nih.gov/compare/)[28] allows us to assume biochemical mechanisms of action for the novel compounds on the basis of their in vitro activity profiles when comparing with those of standard agents. We performed COMPARE computations for synthesized highly active compounds against the NCI "Standard Agents" database at the GI_{50} and TGI levels.

COMPARE analysis hypothesis precludes that the compound may have the same mechanism of action as an agent with a known action mechanism. Most of the significant correlations of tested compounds, in particular for 3-[2-(3,5-diaryl-4,5-dihydropyrazol-1-yl)-4-oxo-4,5-dihydro-1,3-thiazol-5-ylidene]-2,3-dihydro-1*H*-indol-2-ones, have been found with echinomycin and bruceantin (inhibitors of protein or RNA synthesis). Interestingly, mean graph fingerprints of compounds **1**, **4**, **9**, **19** showed significant similarity at the TGI level with tamoxifen (antagonist of the estrogen receptor) in the COMPARE test (Table 4).

CONCLUSIONS

In the present paper the novel 3-[2-(3,5-diaryl-4,5-dihydropyrazol-1-yl)-4-oxo-4,5-dihydro-1,3-thiazol-5-ylidene]-2,3-dihydro-1*H*-indol-2-ones **1**−**23** and 3-(3,5-diarylpyrazol-1-yl)-2,3-dihydro-1*H*-indol-2-ones **24**−**39** were described. Most of these novel compounds were found to possess in vitro human tumor cell line activity substantially more potent than the recently reported antitumor 4-(3,5-diaryl-4,5-dihydro-1*H*-pyrazol-1-yl)-1,3-thiazol-2(5*H*)-ones. The nonthiazolidine derivatives **24**−**39** were far less active than conjugates with three heterocycles, **1**−**20**, emphasizing the importance of the presence and positioning of a central linker (4-thiazolidinone moiety) between two terminal heterocycles (indolone and pyrazoline). The most potent compound, **10**, in the series of pyrazoline−thiazolidinone−isatin conjugates exhibits a mean GI_{50} value of 0.071 μM and a mean TGI value of 0.76 μM in the NCI 60-cell-line screen with a low toxicity and moderate activity level in the in vivo hollow fiber assay.

EXPERIMENTAL SECTION

Chemistry. The starting 3,5-diaryl-2-pyrazolines[29] and 3,5-diaryl-1-thiocarbamoyl-2-pyrazolines[30] were obtained according to the methods described previously.

Melting points were measured in open capillary tubes on a Büchi B-545 melting point apparatus and are uncorrected. The elemental analyses (C, H, N) were performed using the Perkin-Elmer 2400 CHN analyzer. Analysis results indicated by the symbols of the elements or functions were within ±0.4% of the theoretical values. The ^{1}H NMR spectra were recorded on a Varian Gemini 400 MHz spectrometer and ^{13}C NMR spectra on a Varian Mercury-400 100 MHz spectrometer in DMSO-d_6 or DMSO-d_6 + CCl_4 mixture using tetramethylsilane (TMS) as an internal standard. Chemical shifts are reported in ppm units with use of the δ scale. Mass spectra were obtained using electrospray (ES) ionization techniques on an Agilent 1100 series LCMS instrument. Analytical HPLC was performed on an Agilent 1100 HPLC instrument with DAD (diode array detection). ESI refers to electrospray ionization. HPLC refers to high pressure liquid chromatography. LCMS refers to liquid chromatography coupled with mass spectrometry. M in the context of mass spectrometry refers to the molecular peak, and MS refers to mass spectrometry. The purity of all compounds was determined to be ≥95% by HPLC (Agilent 1100 HPLC instrument) with diode array detection. The peak purity was checked with UV spectra.

General Procedure for Synthesis of 3-[2-(3,5-Diaryl-4,5-dihydropyrazol-1-yl)-4-oxo-4,5-dihydro-1,3-thiazol-5-ylidene]-2,3-dihydro-1*H*-indol-2-ones (1−23). A mixture of 3,5-diaryl-1-thiocarbamoyl-2-pyrazoline (10 mmol), chloroacetic acid (10 mmol), appropriate isatin (12 mmol), and anhydrous sodium acetate (20 mmol) was refluxed for 5 h in glacial acetic acid (10 mL). The precipitate that was obtained upon cooling was filtered off, washed with water and methanol, and recrystallized with DMF/ethanol mixtures (1:2 vol).

3-{2-[5-(2-Hydroxyphenyl)-3-phenyl-4,5-dihydropyrazol-1-yl]-4-oxo-4,5-dihydro-1,3-thiazol-5-ylidene}-2,3-dihydro-1*H*-indol-2-one (1). Yield 69%, mp 310−313 °C. ^{1}H NMR (400 MHz, DMSO-d_6 + CCl_4): δ 11.15 (s, 1H), 9.92 (s, 1H), 8.92 (d, J = 7.6 Hz, 1H), 7.92 (d, J = 7.6 Hz, 2H), 7.54−7.59 (m, 3H), 7.35 (t, J = 7.6 Hz, 1H), 7.15 (t, J = 7.7 Hz, 1H), 7.02−7.06 (m, 2H), 6.92 (d, J = 7.5 Hz, 1H), 6.87 (d, J = 8.0 Hz, 1H), 6.78 (t, J = 7.5 Hz, 1H), 5.97 (dd, J = 11.2, 3.9 Hz, 1H), 4.13 (dd, J = 17.9, 11.2 Hz, 1H), 3.41 (dd, J = 17.9, 3.9 Hz, 1H). ^{13}C NMR (100 MHz, DMSO-d_6): δ 179.5 (C═O), 173.1 (C═O), 169.5 (C═N, thiaz), 163.0 (C═N, pyraz), 154.9 (C−OH), 143.6, 137.7, 132.2, 132.1, 130.2, 129.5, 128.5, 127.9, 127.7, 126.3, 125.9, 122.3, 120.9, 119.5, 116.2, 110.6, 61.5 (C$\underline{\text{C}}$HCH$_2$), 42.7 (CH$\underline{\text{C}}$H$_2$). LCMS (ESI +) m/z 467 (M + H)$^+$. Anal. Calcd for $C_{26}H_{18}N_4O_3S$: C, 66.94; H, 3.89; N, 12.01. Found: C, 67.10; H, 3.73; N, 11.87.

3-{2-[3,5-Bis-(4-methoxyphenyl)-4,5-dihydropyrazol-1-yl]-4-oxo-4,5-dihydro-1,3-thiazol-5-ylidene}-5-bromo-2,3-dihydro-1*H*-indol-2-one (7). Yield 80%, mp 316−318 °C. ^{1}H NMR (400 MHz, DMSO-d_6 + CCl_4): δ 11.02 (s, 1H), 9.08 (s, 1H), 7.81 (d, J = 8.8 Hz, 2H), 7.49 (d, J = 7.5 Hz, 1H), 7.24 (d, J = 8.7 Hz, 2H), 7.04 (d, J = 8.8 Hz, 2H), 6.89−6.96 (m, 3H), 5.90 (dd, J = 10.6, 3.8 Hz, 1H), 4.15 (dd, J = 18.6, 10.6 Hz, 1H), 3.83 (s, 3H), 3.71 (s, 3H), 3.52 (dd, J = 18.6, 3.8 Hz, 1H). ^{13}C NMR (100 MHz, DMSO-d_6): δ 179.4 (C═O), 173.2 (C═O), 169.1 (C═N, thiaz), 163.1 (C═N, pyraz), 162.7 (C−O), 159.5 (C−O), 142.1, 139.4, 132.5, 131.3, 130.0, 127.9, 127.8, 126.1, 125.1, 122.5, 122.1, 115.0, 114.8, 111.9, 63.8 (C$\underline{\text{C}}$HCH$_2$), 56.1 (OCH$_3$), 55.7 (OCH$_3$), 43.7 (CH$\underline{\text{C}}$H$_2$). LCMS (ESI+) m/z 589/591 (M + H)$^+$. Anal. Calcd for $C_{28}H_{21}BrN_4O_4S$: C, 57.05; H, 3.59; N, 9.50. Found: C, 57.21; H, 3.67; N, 9.43.

5-Bromo-3-{2-[5-(4-methoxyphenyl)-3-naphthalen-2-yl-4,5-dihydropyrazol-1-yl]-4-oxo-4,5-dihydro-1,3-thiazol-5-ylidene}-2,3-dihydro-1*H*-indol-2-one (10). Yield 67%, mp 283−286 °C. ^{1}H NMR (400 MHz, DMSO-d_6 + CCl_4): δ 11.10 (s, 1H), 9.12 (s, 1H), 8.40 (s, 1H), 7.99−8.08 (m, 4H), 7.61−7.64 (m, 2H), 7.49 (d, J = 7.5 Hz, 1H), 7.29 (d, J = 7.6 Hz, 2H), 6.94 (d, J = 7.6 Hz, 2H), 6.89 (d, J = 8.0 Hz, 1H), 5.98 (dd, J = 10.9, 2.3 Hz, 1H), 4.29 (dd, J = 17.9, 10.9 Hz, 1H), 3.76 (s, 3H), 3.66 (dd, J = 17.9, 2.3 Hz, 1H). ^{13}C NMR (100 MHz, DMSO-d_6): δ 179.5 (C═O), 173.6 (C═O), 169.5 (C═N, thiaz),

dx.doi.org/10.1021/jm300789g | J. Med. Chem. 2012, 55, 8630−8641

Table 3. Influence of Compound 10 on the Growth of Individual Tumor Cell Lines

		GI_{50}, μM		TGI, μM		LC_{50}, μM	
disease	cell line	1[a]	2[b]	1[a]	2[b]	1[a]	2[b]
leukemia	CCRF-CEM	0.227	0.0329	11.0	0.483	>100.0	>100.0
	HL-60 (TB)	0.558	0.257	11.5	3.2	>100.0	49.3
	K-562	0.28	0.037	>100.0	12.4	>100.0	>100.0
	MOLT-4	0.239	0.0307	2.94	0.521	>100.0	>100.0
	RPMI-8226	1.03	0.214	26.8	1.4	>100.0	42.2
	SR	0.0666	0.0289	1.18	0.13	>100.0	>100.0
NSC lung cancer	A549/ATCC	0.0375	0.0247	0.178	0.0695	25.7	33.3
	EKVX	0.0734	0.0476	0.426	0.48	>100.0	>100.0
	HOP-62	0.221	0.022		0.0498	>100.0	0.157
	HOP-92	0.0153	<0.01	0.443	0.0242	14.5	1.47
	NCI-H226	0.0215	0.0406	0.582	0.173	4.26	0.586
	NCI-H23	0.0548	0.0246	0.246	0.0567		0.291
	NCI-H322M	0.189	0.036	2.96	0.56	>100.0	64.1
	NCI-H460	0.0571	0.0331	0.25	0.112		5.45
	NCI-H522	0.124		0.288			
colon cancer	COLO 205	0.139	0.021		0.042	>100.0	0.0841
	HCC-2998	0.0869	0.0252	0.246	0.0658	0.641	0.272
	HCT-116	0.0448	0.018		0.0335	>100.0	0.0624
	HCT-15	0.286	0.0629	1.25	0.325	>100.0	2.45
	HT29	0.199		0.537			
	KM12	0.117	0.0231	0.265	0.0535	0.601	0.231
	SW-620	0.0229	0.022	0.0493	0.0477	0.127	0.13
CNS cancer	SF-268	0.0738	0.0365	0.47	0.222	26.3	9.63
	SF-295	0.0265	0.0285	0.0786	0.0943	1.17	4.58
	SF-539	0.157	0.0231	0.442	0.0542		0.296
	SNB-19	0.292	0.0385	12.2	0.411	61.1	8.98
	SNB-75	0.13	0.0159	0.411	0.0343	>100.0	0.0698
	U251	0.0289	0.0246	0.0726	0.0578	0.289	0.664
melanoma	LOX IMVI	0.0862	0.0243		0.0589		0.249
	MALME-3M	0.145	0.0277	0.357	0.0729		0.64
	M14	0.198	0.0245		0.0593	>100.0	0.21
	MDA-MB-435	0.0401	0.0318	0.188	0.106		2.44
	SK-MEL-2	0.22		0.044		0.882	
	SK-MEL-28	0.327	0.0218		0.0515	>100.0	0.205
	SK-MEL-5	0.137	0.0315	0.266	0.0106	0.517	0.341
	UACC-257	0.237	0.0511	0.686	0.318		>100.0
	UACC-62	0.206	0.0547	0.551	0.261	79.6	1.19
ovarian cancer	IGROV1	0.289	0.0498	1.66	0.451	>100.0	>100.0
	OVCAR-3	0.101	0.0216	0.252	0.045	0.628	0.0937
	OVCAR-4	0.215	0.0326	>100.0	0.111	>100.0	>100.0
	OVCAR-5	0.1975	0.0336	0.587	0.131	29.2	2.11
	OVCAR-8	0.0587	0.032	0.486	0.176	28.7	24.1
	NCI/ADR-RES	0.675	1.59	>100.0		>100.0	>100.0
	SK-OV-3	0.319	0.033	>100.0	0.114	>100.0	2.84
renal cancer	786-0	0.072	0.0194		0.0387	>100.0	0.0772
	A498	0.151	0.0251	0.313	0.0786	0.65	0.316
	ACHN	0.0637	0.0267	37.8	0.0646	>100.0	32.3
	CAKI-1	0.151	0.0965	0.608	1.74	>100.0	>100.0
	RXF 393	0.0543	0.0197	0.202	0.0403	0.55	0.0822
	SN12C	0.171	0.0434	0.588	0.223		1.7
	TK-10	0.17		0.522		>100.0	
	UO-31	0.206	0.0578				
prostate cancer	PC-3	0.229	0.026	0.778	0.0827	5.46	6.84
	DU-145	0.0669	0.0393	0.752	1.34	25.5	38.0
breast cancer	MCF7	0.0557	0.0264	>100.0	0.0747	>100.0	0.586
	MDA-MB-231/ATCC	0.0145	0.025		0.0627		0.349
	HS 578T	0.0644	0.0774	1.03	>100.0	>100.0	>100.0
	BT-549	0.553		7.74		35.1	
	T-47D	0.127	0.0236		0.0611		

dx.doi.org/10.1021/jm300789g | J. Med. Chem. 2012, 55, 8630−8641

Table 3. continued

disease	cell line	GI_{50}, μM		TGI, μM		LC_{50}, μM	
		1[a]	2[b]	1[a]	2[b]	1[a]	2[b]
	MDA-MB-468	0.0913	0.0223	0.222	0.0622	0.508	0.19

[a]First evaluation. [b]Second evaluation.

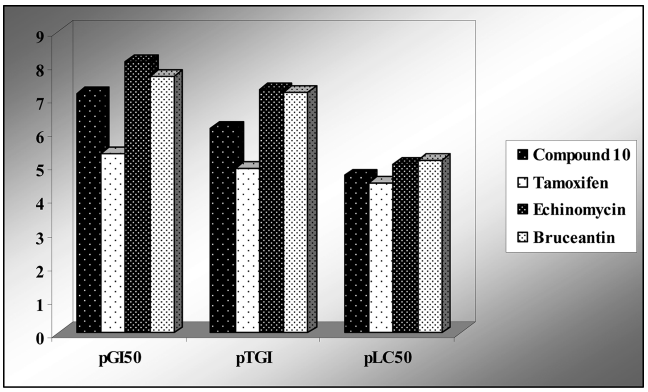

Figure 6. Anticancer activity of the most active compound **10** in comparison with standard agents.

162.9 (C═N, pyraz), 159.5 (C−O), 143.7, 139.4, 134.4, 133.1, 132.2, 132.1, 129.7, 129.3, 129.1, 128.6, 128.4, 128.3, 127.9, 127.6, 127.4, 126.7, 123.7, 122.1, 120.9, 114.8, 110.6, 64.0 ($\underline{C}HCH_2$), 55.6 (OCH_3), 43.8 ($CH\underline{C}H_2$). LCMS (ESI+) m/z 609/611 $(M + H)^+$. Anal. Calcd for $C_{31}H_{21}BrN_4O_3S$: C, 61.09; H, 3.47; N, 9.19. Found: C, 61.25; H, 3.62; N, 9.33.

1-Methyl-3-[4-oxo-2-(3-phenyl-5-thiophen-2-yl-4,5-dihydropyrazol-1-yl)-4*H*-thiazol-5-ylidene]-2,3-dihydro-1*H*-indol-2-one (23). Yield 72%, mp 248−250 °C. ^{1}H NMR (400 MHz, DMSO-d_6 + CCl_4): δ 8.96 (d, J = 7.7 Hz, 1H), 7.94 (d, J = 7.4 Hz, 2H), 7.56−7.63 (m, 3H), 7.50 (d, J = 4.2 Hz, 1H), 7.42 (t, J = 7.1 Hz, 1H), 7.22 (d, J = 2.7 Hz, 1H), 7.11 (t, J = 7.7 Hz, 1H), 7.06 (d, J = 7.8 Hz, 1H), 7.02 (t, J = 4.2 Hz, 1H), 6.28 (dd, J = 10.6, 2.8 Hz, 1H), 4.18 (dd, J = 18.3, 10.6 Hz, 1H), 3.72 (dd, J = 18.3, 2.8 Hz, 1H), 3.28 (s, 3H). ^{13}C NMR (100 MHz, DMSO-d_6): δ 179.2 (C═O), 173.5 (C═O), 167.9 (C═N, thiaz), 162.8 (C═N, pyraz), 144.2, 142.3, 137.8, 132.5, 132.2, 129.9, 129.6, 128.3, 128.1, 127.5, 126.7, 126.6, 125.7, 122.9, 120.1, 109.4, 59.9 ($\underline{C}HCH_2$), 43.6 ($CH\underline{C}H_2$), 26.9 (CH_3). LCMS (ESI+) m/z 471 $(M + H)^+$. Anal. Calcd for $C_{25}H_{18}N_4O_2S_2$: C, 63.81 H, 3.86; N, 11.91. Found: C, 63.69; H, 3.95; N, 11.81.

Crystal Data. $C_{25}H_{18}N_4O_2S_2$, M_r = 470.55, triclinic, space group $P\bar{1}$ a = 8.8197(9) Å, b = 10.7567(11) Å, c = 12.0420(12) Å, α = 94.037(8)°, β = 108.803(9)°, γ = 101.738(9)°, V = 1047.39(18) Å^3, Z = 2, D_{calc} = 1.492 g/cm^3, μ = 2.578 mm^{-1}, T = 130(2) K.

Data Collection. A brown plate crystal (DMF) of 0.30 mm × 0.20 mm × 0.03 mm was used to record 7343 (Cu Kα radiation, θ_{max} = 73.5°) intensities on an Oxford Diffraction SuperNova four-circle diffractometer equipped with an Atlas CCD detector[31] using mirror-monochromatized Cu Kα radiation from a high-flux microfocus source (λ = 1.541 78 Å). Accurate unit cell parameters were determined by least-squares techniques from the θ values of 2906 reflections, θ range 3.9−73.5°. The data were corrected for Lorentz polarization and for absorption effects.[31] The 4052 total unique reflections (R_{int} = 0.0258) were used for structure determination.

Structure Solution and Refinement. The structure was solved by direct methods using the program SHELXS-97, and refinement was done against F^2 for all data using SHELXL-97.[32] The H atoms were positioned geometrically and were refined with a riding model, and U_{iso}(H) values were constrained to be 1.2 (1.5 for methyl group) times U_{eq} of the appropriate carrier atom. The methyl H atoms were refined as a rigid group that was allowed to rotate. The final refinement converged with R = 0.0578 (for 3532 data with $F^2 > 4\sigma(F^2)$), wR = 0.1656 (on F^2 for all data), and S = 1.062 (on F^2 for all data). The largest difference peak and hole was 0.869 and −0.417 e Å^{-3}. Crystals **23** were twinned, hence the lower accuracy of the final results. The molecular illustration was drawn using ORTEP-3 for Windows.[33]

The supplementary crystallographic data are deposited at the Cambridge Crystallographic Data Centre (CCDC), 12 Union ROAD, Cambridge CB2 1EZ (U.K.) (phone, (+44) 1223/336-408; fax, (+44) 1223/336-033; e-mail, deposit@ccdc.cam.ac.uk; World Wide Web, http://www.ccdc.cam.ac.uk (deposition no. CCDC 859413)).

General Procedure for Synthesis of 3-[3,5-Diarylpyrazol-1-yl]-2,3-dihydro-1*H*-indol-2-ones (24−39). A mixture of 3,5-diarylpyrazoline (5 mmol) and appropriate isatin (5 mmol) was refluxed for 1 h in ethanol (15 mL). The obtained precipitate was filtered off, washed with ethanol, and recrystallized with DMF/ethanol mixture (1:2 vol).

{3-[5-(2-Hydroxyphenyl)-3-phenylpyrazol-1-yl]-2-oxo-2,3-dihydroindol-1-yl}acetic Acid (24). Yield 78%, mp 132−134 °C. ^{1}H NMR (400 MHz, DMSO-d_6 + CCl_4): δ 13.14 (s, 1H), 10.25 (s, 1H), 7.70 (d, J = 7.4 Hz, 1H), 7.27−7.42 (m, 8H), 7.09 (t, J = 8.7 Hz, 2H), 6.98−7.07 (m, 2H), 6.84 (s, 1H), 5.79 (s, 1H), 4.52 (d, J = 18.2 Hz, 1H), 4.47 (d, J = 18.2 Hz, 1H). ^{13}C NMR (100 MHz, DMSO-d_6): δ 172.0 (C═O), 169.5 (COOH), 155.4 (C−O), 151.5 (C═N), 143.8, 133.4, 123.3, 131.3, 130.0, 129.0, 128.2, 125.8, 125.7, 125.3, 123.1, 119.9, 117.1, 116.7, 109.8, 104.5, 60.7 (CH), 56.6 (CH_2). LCMS (ESI+) m/z 426 $(M + H)^+$. Anal. Calcd for $C_{25}H_{19}N_3O_4$: C, 70.58; H, 4.50; N, 9.88. Found: C, 70.75; H, 4.69; N, 9.72.

Crystal Data. $C_{25}H_{19}N_3O_4$,2(C_2H_6O), M_r = 517.57, triclinic, space group $P\bar{1}$, a = 11.5227(7) Å, b = 11.8942(7) Å, c = 12.2739(8) Å, α = 113.837(6)°, β = 115.349(6)°, γ = 93.313(5)°, V = 1335.22(14) Å^3, Z = 2, D_{calc} = 1.287 g/cm^3, μ = 0.091 mm^{-1}, T = 130(2) K.

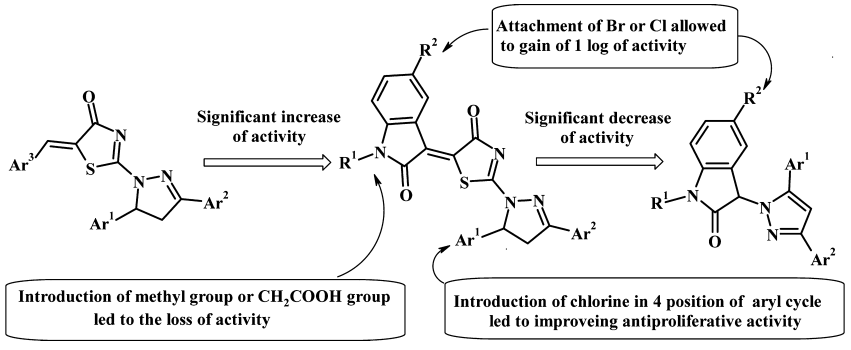

Figure 7. SAR analysis of the noncondensed heterocyclic compounds with 4-thiazolidinone, 2,3-dihydro-1*H*-indol-2-one, and pyrazole or pyrazoline moieties.

dx.doi.org/10.1021/jm300789g | J. Med. Chem. 2012, 55, 8630−8641

Table 4. COMPARE Analysis Results for Highly Active Compounds

compd	end point	PCC[a]	target	target vector NSC	target mechanism of action[b]
1	TGI	0.555	tamoxifen	S180973	antagonist of the estrogen receptor
		0.553	5-azacytidine	S102816	DNA/RNA antimetabolite
3	TGI	0.565	actinomycin D	S3053	DNA transcription inhibitor
		0.565	anthrapyrazole	S355644	topoisomerase II inhibitor
		0.559	chromomycin A3	S58514	RNA polymerase inhibitor
4	GI_{50}	0.686	echinomycin	S526417	inhibitor of RNA synthesis
	TGI	0.628	bruceantin	S165563	inhibitor of protein synthesis
		0.617	tamoxifen	S180973	antagonist of the estrogen receptor
6	GI_{50}	0.634	nitroimidazole	S314055	
		0.570	nitroestrone	S321803	
	TGI	0.555	*R*-methylformamide	S3051	
7	GI_{50}	0.550	echinomycin	S526417	inhibitor of RNA synthesis
	TGI	0.595	acodazole hydrochloride	S305884	
8	GI_{50}	0.595	echinomycin	S526417	inhibitor of RNA synthesis
	TGI	0.631	acodazole hydrochloride	S305884	
		0.553	bruceantin	S165563	inhibitor of protein synthesis
9	TGI	0.549	tamoxifen	S180973	antagonist of the estrogen receptor
10	GI_{50}	0.744	echinomycin	S526417	inhibitor of RNA synthesis
		0.724	bruceantin	S165563	inhibitor of protein synthesis
		0.705	actinomycin D	S3053	DNA transcription inhibitor
		0.693	chromomycin A3	S58514	RNA polymerase inhibitor
		0.612	deoxydoxorubicin	S267469	topoisomerase II inhibitor
		0.576	acodazole hydrochloride	S305884	
	TGI	0.664	tetrocarcin A sodium salt	S333856	
14	TGI	0.559	bruceantin	S165563	inhibitor of protein synthesis
15	GI_{50}	0.589	echinomycin	S526417	inhibitor of RNA synthesis
		0.553	bruceantin	S165563	inhibitor of protein synthesis
	TGI	0.627	bruceantin	S165563	inhibitor of protein synthesis
		0.593	acodazole hydrochloride	S305884	
17	GI_{50}	0.748	echinomycin	S526417	inhibitor of RNA synthesis
		0.596	bruceantin	S165563	inhibitor of protein synthesis
		0.564	chromomycin A3	S58514	RNA polymerase inhibitor
19	TGI	0.797	tamoxifen	S180973	antagonist of the estrogen receptor
		0.603	hycanthone	S142982	alkylating agent

[a]Only correlations with Pearson correlation coefficient PCC ≥ 0.55 were selected, as significant. [b]Putative mechanisms of action were identified with the use of literature sources.

Data Collection. A colorless block crystal (ethanol) of 0.40 mm × 0.40 mm × 0.20 mm was used to record 16 524 (Mo Kα radiation, θ_{max} = 29.1°) intensities on an Xcalibur-Atlas diffractometer.[34] The data were corrected for Lorentz polarization and for absorption effects.[34] Accurate unit-cell parameters were determined by a least-squares fit of 9535 reflections of highest intensity, chosen from the whole experiment. The 6388 total unique reflections (R_{int} = 0.0188) were used for structure determination.

Structure Solution and Refinement. The structure was solved by direct methods using SHELXS-97, and refinement was done against F^2 for all data using SHELXL-97.[32] The positions of the H atoms bonded to O13, O32, and O33 atoms were obtained from the difference Fourier map and were refined freely. The remaining H atoms were placed in geometrically calculated positions and were refined using a riding model, with C−H = 0.96 Å (CH_3), 0.97 Å (CH_2), 0.98 Å ($C_{sp^3}H$), 0.93 Å ($C_{ar}H$) and $U_{iso}(H) = 1.2U_{eq}(C)$ or $1.5U_{eq}(C)$ for methyl H atoms. The methyl groups were refined as rigid groups, which were allowed to rotate. The alternative positions of C/O atoms of the disordered solvent molecule, designated as A and B, were constrained to have the same U_{ij} components. The sum of site-occupancy factors for the disordered molecule was constrained to unity. The final refinement converged with R = 0.0370 (for 5016 data with $F^2 > 4\sigma(F^2)$), wR = 0.1034 (on F^2 for all data), and S = 1.081 (on F^2 for all data). The largest difference peak and hole was 0.293 and −0.237 e Å^{-3}. The molecular illustration was drawn using ORTEP-3 for Windows.[33]

The supplementary crystallographic data are deposited at the Cambridge Crystallographic Data Centre (CCDC), 12 Union ROAD, Cambridge CB2 1EZ (U.K.) (phone, (+44) 1223/336-408; fax, (+44) 1223/336-033; e-mail, deposit@ccdc.cam.ac.uk, World Wide Web, http://www.ccdc.cam.ac.uk (deposition no. CCDC 859414)).

3-[3,5-Bis(4-methoxyphenyl)pyrazol-1-yl]-2,3-dihydro-1*H*-indol-2-one (25). Yield 83%, mp 216−219 °C. ^{1}H NMR (400 MHz, DMSO-d_6 + CCl_4): δ 10.68 (s, 1H), 7.58−7.65 (m, 4H), 7.28 (t, J = 7.4 Hz, 1H), 7.10−7.12 (m, 3H), 6.92−6.98 (m, 4H), 6.81 (s, 1H), 5.95 (s, 1H), 3.82 (s, 3H), 3.76 (s, 3H). ^{13}C NMR (100 MHz, DMSO-d_6): δ 174.0 (C═O), 160.2 (C−O), 159.5 (C−O), 151.1 (C═N), 147.0, 143.1, 130.8, 129.9, 127.2, 127.1, 125.9, 124.7, 122.4, 122.3, 114.9, 114.5, 110.6, 60.6 (C−N), 55.8 (OCH_3), 55.6 (OCH_3). LCMS (ESI+) m/z 412 $(M + H)^+$. Anal. Calcd for $C_{25}H_{21}N_3O_3$: C, 72.98; H, 5.14; N, 10.21. Found: C, 73.06; H, 5.01; N, 10.32.

3-[5-(4-Methoxyphenyl)-3-naphthalen-2-ylpyrazol-1-yl]-2,3-dihydro-1*H*-indol-2-one (35). Yield 80%, mp 208−211 °C. ^{1}H NMR (400 MHz, DMSO-d_6 + CCl_4): δ 10.72 (s, 1H), 8.27 (s, 1H), 7.91−7.96 (m, 4H), 7.62 (br s, 1H), 7.47−7.52 (m, 2H), 7.31 (t, J = 7.6 Hz, 1H), 7.13−7.16 (m, 3H), 7.05 (s, 1H), 6.94−6.99 (m, 2H), 6.03 (s, 1H), 3.84 (s, 3H). ^{13}C NMR (100 MHz, DMSO-d_6): δ 173.9 (C═O), 160.4 (C−O), 151.2 (C═N), 143.1, 133.6, 133.1, 130.8, 130.7, 129.9, 128.6, 128.5, 128.1, 127.1, 126.8, 126.5, 124.8, 124.2, 124.1, 122.5, 122.3, 114.9, 110.6, 55.8 (OCH_3). LCMS (ESI+) m/z 432 $(M + H)^+$. Anal. Calcd for $C_{28}H_{21}N_3O_2$: C, 77.94; H, 4.91; N, 9.74. Found: C, 77.81; H, 4.86; N, 9.52.

dx.doi.org/10.1021/jm300789g | J. Med. Chem. 2012, 55, 8630−8641

Pharmacology. A primary anticancer assay was performed for an approximately 60 human tumor cell line panel derived from nine neoplastic diseases, in accordance with the protocol of the Drug Evaluation Branch, National Cancer Institute, Bethesda, MD.[26] Tested compounds were added to the culture at a single concentration (10^{-5} M), and the cultures were incubated for 48 h. End point determinations were made with a protein binding dye, sulforhodamine B (SRB). The results for each tested compound were reported as the growth percentage of the treated cells when compared to that of the untreated control cells. The percentage growth was evaluated spectrophotometrically versus controls not treated with test agents. The cytotoxic and/or growth inhibitory effects of the most active selected compounds were tested in vitro against the full panel of about 60 human tumor cell lines at 10-fold dilutions of five concentrations ranging from 10^{-4} to 10^{-8} M. A 48 h continuous drug exposure protocol was followed, and an SRB protein assay was used to estimate cell viability or growth.

By use of the seven absorbance measurements [time zero, (T_z), control growth in the absence of drug (C), and test growth in the presence of drug at the five concentration levels (T_i)], the percentage growth was calculated at each of the drug concentrations levels. Percentage growth inhibition was calculated as

$$[(T_i - T_z)/(C - T_z)] \times 100 \quad \text{for concentrations for which } T_i \geq T_z$$

$$[(T_i - T_z)/T_z] \times 100 \quad \text{for concentrations for which } T_i < T_z$$

Three dose response parameters (GI_{50}, TGI, LC_{50}) were calculated for each compound. Growth inhibition of 50% (GI_{50}) was calculated from $[(T_i - T_z)/(C - T_z)] \times 100 = 50$, which was the drug concentration resulting in a 50% lower net protein increase in the treated cells (measured by SRB staining) compared to the net protein increase seen in the control cells. The drug concentration resulting in total growth inhibition (TGI) was calculated from $T_i = T_z$. The LC_{50} (concentration of drug resulting in a 50% reduction in the measured protein at the end of the drug treatment compared to that at the beginning) indicating a net loss of cells following treatment was calculated from $[(T_i - T_z)/T_z] \times 100 = -50$. Values were calculated for each of these three parameters if the level of activity was reached; however, if the effect was not reached or was exceeded, the value for that parameter was expressed as more or less for the maximum or minimum concentration tested. The lowest values are obtained with the most sensitive cell lines. The compounds having $GI_{50} \leq 100$ μM were declared to be active.

■ ASSOCIATED CONTENT

Supporting Information

X-ray details and characterization data for compounds **2**−**6**, **8**, **9**, **11**−**23**, **26**−**34**, and **36**−**39**. This material is available free of charge via the Internet at http://pubs.acs.org.

■ AUTHOR INFORMATION

Corresponding Author

*Phone: +38 0322 75-59-66. Fax: +38 0322 75-77-34. E-mail: dr_r_lesyk@org.lviv.net.

Notes

The authors declare no competing financial interest.

■ ACKNOWLEDGMENTS

We are grateful to Dr. V. L. Narayanan from Drug Synthesis and Chemistry Branch, National Cancer Institute, Bethesda, MD, U.S., for in vitro evaluation of the anticancer activity.

■ ABBREVIATIONS USED

JSP-1, JNK-stimulating phosphatase 1; SHP-2, nonmembrane protein tyrosine phosphatase 2; CAI, carbonic anhydrase isozyme; SRB, sulforhodamine B; PCC, Pearson correlation coefficient; GI_{50}, molar concentration of the compound that inhibits 50% net cell growth; LC_{50}, molar concentration of the compound leading to 50% net cell death; TGI, molar concentration of the compound leading to total inhibition

■ REFERENCES

(1) (a) Lesyk, R.; Zimenkovsky, B. 4-Thiazolidones: Centenarian History, Current Status and Perspectives for Modern Organic and Medicinal Chemistry. *Curr. Org. Chem.* **2004**, *8*, 1547−1577. (b) Havrylyuk, D.; Zimenkovsky, B.; Lesyk, R. Synthesis and Anticancer Activity of Novel Nonfused Bicyclic Thiazolidinone Derivatives. *Phosphorus, Sulfur Silicon Relat. Elem.* **2009**, *184*, 638−650. (c) Kaminskyy, D.; Khyluk, D.; Vasylenko, O.; Lesyk, R. An Efficient Method for the Transformation of 5-Ylidenerhodanines into 2,3,5-Trisubstituted-4-thiazolidinones. *Tetrahedron Lett.* **2012**, *53*, 557−559. (d) Kaminskyy, D.; Khyluk, D.; Vasylenko, O.; Zaprutko, L.; Lesyk, R. A Facile Synthesis and Anticancer Activity Evaluation of Spiro[thiazolidinone-isatin] Conjugates. *Sci. Pharm.* **2011**, *79*, 763−777. (e) Lesyk, R. B.; Zimenkovsky, B. S.; Kaminskyy, D. V.; Kryshchyshyn, A. P.; Havrylyuk, D. Ya.; Atamanyuk, D. V.; Subtel'na, I. Yu.; Khyluk, D. V. Thiazolidinone Motif in Anticancer Drug Discovery. Experience of DH LNMU Medicinal Chemistry Scientific Group. *Biopolym. Cell* **2011**, *27*, 107−117. (f) Kaminskyy, D.; Zimenkovsky, B.; Lesyk, R. Synthesis and in Vitro Anticancer Activity of 2,4-Azolidinedione-acetic Acids Derivatives. *Eur. J. Med. Chem.* **2009**, *44*, 3627−3636.

(2) Kumar, S.; Bawa, S.; Drabu, S; Kumar, R.; Gupta, H. Biological Activities of Pyrazoline Derivatives—A Recent Development. *Recent Pat. Anti-Infect. Drug Discovery* **2009**, *4*, 154−163.

(3) Pandeya, S. N.; Smitha, S.; Jyoti, M.; Sridhar, S. K. Biological Activities of Isatin and Its Derivatives. *Acta Pharm.* **2005**, *55*, 27−46.

(4) Cutshall, N. S.; O'Day, C.; Prezhdo, M. Rhodanine Derivatives as Inhibitors of JSP-1. *Bioorg. Med. Chem. Lett.* **2005**, *15*, 3374−3379.

(5) Carter, P. H.; Scherle, P. A.; Muckelbauer, J. A.; Voss, M. E.; Liu, R.-Q.; Thompson, L. A.; Tebben, A. J.; Solomon, K. A.; Lo, Y. C.; Li, Z.; Strzemienski, P.; Yang, G.; Falahatpisheh, N.; Xu, M.; Wu, Z.; Farrow, N. A.; Ramnarayan, K.; Wang, J.; Rideout, D.; Yalamoori, V.; Domaille, P.; Underwood, D. J.; Trzaskos, J. M.; Friedman, S. M.; Newton, R. C.; Decicco, C. P. Photochemically Enhanced Binding of Small Molecules to the Tumor Necrosis Factor Receptor-1 Inhibits the Binding of TNF-α. *Proc. Natl. Acad. Sci. U.S.A.* **2001**, *98* (21), 11879−11884.

(6) Degterev, A.; Lugovskoy, A.; Cardone, M.; Mulley, B.; Wagner, G.; Mitchison, T.; Yuan, J. Identification of Small-Molecule Inhibitors of Interaction between the BH3 Domain and Bcl-xl. *Nat. Cell Biol.* **2001**, *3* (2), 173−182.

(7) Dayam, R.; Aiello, F.; Deng, J.; Wu, Y.; Garofalo, A.; Chen, X.; Neamati, N. Discovery of Small Molecule Integrin $\alpha_v\beta_3$ Antagonists as Novel Anticancer Agents. *J. Med. Chem.* **2006**, *49*, 4526−4534.

(8) Geronikaki, A.; Eleftheriou, P.; Vicini, P.; Alam, I.; Dixit, A.; Saxena, A. K. 2-Thiazolylimino/heteroarylimino-5-arylidene-4-thiazolidinones as New Agents with SHP-2 Inhibitory Action. *J. Med. Chem.* **2008**, *51*, 5221−5228.

(9) Ma, J.; Li, S.; Reed, K.; Guo, P.; Gallo, J. M. Pharmacodynamic-Mediated Effects of the Angiogenesis Inhibitor SU5416 on the Tumor Disposition of Temozolomide in Subcutaneous and Intracerebral Glioma Xenograft Models. *J. Pharmacol. Exp. Ther.* **2003**, *305*, 833−839.

(10) Lane, M. E.; Yu, B.; Rice, A.; Lipson, K. E.; Liang, C.; Sun, L.; Tang, C.; McMahon, G.; Pestell, R. G.; Wadler, S. A Novel CDK2-Selective Inhibitor, SU9516, Induces Apoptosis in Colon Carcinoma Cells. *Cancer Res.* **2001**, *61*, 6170−6177.

(11) Andreani, A.; Burnelli, S.; Granaiola, M.; Leoni, A.; Locatelli, A.; Morigi, R.; Rambaldi, M.; Varoli, L.; Landi, L.; Prata, C.; Berridge, M. V.; Grasso, C.; Fiebig, H.-H.; Kelter, G.; Burger, A. M.; Kunkel, M. W. Antitumor Activity of Bis-indole Derivatives. *J. Med. Chem.* **2008**, *51*, 4563−4570.

(12) Abdel-Hamid, M.; Abdel-Hafez, A.; El-Koussi, N.; Mahfouz, N.; Innocenti, A.; Supuran, C. T. Design, Synthesis, and Docking Studies of New 1,3,4-Thiadiazole-2-thione Derivatives with Carbonic Anhydrase Inhibitory Activity. *Bioorg. Med. Chem.* **2007**, *15*, 6975−6984.
(13) Lin, R.; Chiu, G.; Yu, Y.; Connolly, P. J.; Li, S.; Lu, Y.; Adams, M.; Fuentes-Pesquera, A. R.; Emanuela, S. L.; Greenberger, L. M. Design, Synthesis, and Evaluation of 3,4-Disubstituted Pyrazole Analogues as Anti-tumor CDK Inhibitors. *Bioorg. Med. Chem. Lett.* **2007**, *17*, 4557−4561.
(14) Beswick, M. C.; Brough, P. A.; Drysdale, M. J.; Dymock, B. W. 3-(2-Hydroxy-phenyl)-1*H*-pyrazole-4-carboxylic Acid Amide Derivatives as HSP90 Inhibitors for the Treatment of Cancer. US 2007/0112192, 2007.
(15) Abadi, A. H.; Eissa, A. A. H.; Hassan., G. S. Synthesis of Novel 1,3,4-Trisubstituted Pyrazole Derivatives and Their Evaluation as Antitumor and Antiangiogenic Agents. *Chem. Pharm. Bull.* **2003**, *51*, 838−844.
(16) Manna, F.; Chimenti, F.; Fioravantia, R.; Bolasco, A.; Secci, D.; Chimenti, P.; Ferlini, C.; Scambia, G. Synthesis of Some Pyrazole Derivatives and Preliminary Investigation of Their Affinity Binding to P-glycoprotein. *Bioorg. Med. Chem. Lett.* **2005**, *15*, 4632−4635.
(17) (a) Solomon, V. R.; Hu, C.; Lee, H. Hybrid Pharmacophore Design and Synthesis of Isatin−Benzothiazole Analogs for Their Anti-Breast Cancer Activity. *Bioorg. Med. Chem.* **2009**, *17*, 7585−7592. (b) Meunier, B. Hybrid Molecules with a Dual Mode of Action: Dream or Reality? *Acc. Chem. Res.* **2008**, *41*, 69−77.
(18) (a) Havrylyuk, D.; Mosula, L.; Zimenkovsky, B.; Vasylenko, O.; Gzella, A.; Lesyk, R. Synthesis and Anticancer Activity Evaluation of 4-Thiazolidinones Containing Benzothiazole Moiety. *Eur. J. Med. Chem.* **2010**, *45*, 5012−5021. (b) Lesyk, R.; Vladzimirska, O.; Holota, S.; Zaprutko, L.; Gzella, A. New 5-substituted Thiazolo[2,3-*d*][1,2,4]-triazol-6-ones. Synthesis and Anticancer Evaluation. *Eur. J. Med. Chem.* **2007**, *42*, 641−648. (c) Havrylyuk, D.; Kovach, N.; Zimenkovsky, B.; Vasylenko, O.; Lesyk, R. Synthesis and Anticancer Activity of Isatin-Based Pyrazolines and Thiazolidines Conjugates. *Arch. Pharm. Chem. Life Sci.* **2011**, *344*, 514−522. (d) Mosula, L.; Zimenkovsky, B.; Havrylyuk, D.; Missir, A.-V.; Chirita, I. C.; Lesyk, R. Synthesis and Antitumor Activity of Novel 2-Thioxo-4-Thiazolidinones with Benzothiazole Moieties. *Farmacia* **2009**, *57*, 321−330. (e) Kaminskyy, D.; Vasylenko, O.; Atamanyuk, D.; Gzella, A.; Lesyk, R. Isorhodanine and Thiorhodanine Motifs in the Synthesis of Fused Thiopyrano[2,3-*d*][1,3]thiazoles. *Synlett* **2011**, *10*, 1385−1389.
(19) Havrylyuk, D.; Zimenkovsky, B.; Vasylenko, O.; Zaprutko, L.; Gzella, A.; Lesyk, R. Synthesis of Novel Thiazolone-Based Compounds Containing Pyrazoline Moiety and Evaluation of Their Anticancer Activity. *Eur. J. Med. Chem.* **2009**, *44*, 1396−1404.
(20) Havrylyuk, D. Ya.; Zimenkovsky, B. S.; Vasylenko, O. M.; Lesyk, R. B. Synthesis and Evaluation of Antiviral Activity of Thiazolone Derivatives with Pyrazoline Moiety in Molecules. *J. Org. Pharm. Chem.* **2009**, 7 (1), 42−47; *Chem. Abstr.* **2009**, *151*, 491032. (b) Zimenkovsky, B. S.; Devinyak, O. T.; Havrylyuk, D. Ya.; Lesyk, R. B. Analysis of Anticancer Activity of 4-Thiazolidinone Derivatives and Their Classification by Possible Mechanisms of Activity Using Mathematic Modelling Methods. *J. Org. Pharm. Chem.* **2011**, *9* (3), 64−71; *Chem Abstr* **2011**, *156*, 468508.
(21) Bergman, J.; Stalhandske, C.; Vallberg, H. Studies of the Reaction between Indole-2,3-diones (Isatins) and Secondary Aliphatic Amines. *Acta Chem. Scand.* **1997**, *51*, 753−759.
(22) Desenko, S. M.; Chernenko, V. N.; Orlov, V. D.; Musatov, V. I. 22,-Disubstituted 6,6a-dihydro-1*H*-pyrazolo-[1,5-*c*]-benzo[*e*]-1,3-oxazines. *Kharkov Univ. Bull.* **2000**, *29*, 46−49.
(23) Desenko, S. M.; Chernenko, V. N.; Orlov, V. D.; Musatov, V. I. New Oxidation−Reduction Transformation of Derivatives of 1,10b-Dihydro-1*H*-pyrazolo[1,5-*c*]-1,3-benzoxazine and 7,12-Dihydro-6*H*-[1]benzopyrano[4,3-*d*]-1,2,4-triazolo[1,5-*a*]pyrimidine. *Chem. Heterocycl. Compd.* **2001**, *37*, 1312−1313.
(24) Allen, F. H.; Kennard, O.; Watson, D. G.; Brammer, L.; Orpen, A. G.; Taylor, R. Tables of Bond Lengths Determined by X-ray and Neutron Diffraction. Part 1. Bond Lengths in Organic Compounds. *J. Chem. Soc. Perkin Trans. 2* **1987**, S1−19.
(25) Cremer, D.; Pople, J. A. General definition of ring puckering coordinates. *J. Am. Chem. Soc.* **1975**, *97*, 1354−1358.
(26) (a) Monks, A.; Scudiero, D.; Skehan, P.; Shoemaker, R.; Paull, K.; Vistica, D.; Hose, C.; Langley, J.; Cronise, P.; Vaigro-Wolff, A.; Gray-Goodrich, M.; Campbell, H.; Mayo, J.; Boyd, M. Feasibility of a High-Flux Anticancer Drug Screen Using a Diverse Panel of Cultured Human Tumor Cell Lines. *J. Natl. Cancer Inst.* **1991**, *83* (11), 757−766. (b) Boyd, M. R.; Paull, K. D. Some Practical Considerations and Applications of the National Cancer Institute in Vitro Anticancer Drug Discovery Screen. *Drug Dev. Res.* **1995**, *34*, 91−109. (c) Boyd, M. R. The NCI Human Tumour Cell Line (60-Cell): Concept, Implementation, and Applications Screen. In *Anticancer Drug Development Guide*, 2nd ed.; Teicher, B. A., Paul, A. A., Eds.; Humana Press Inc.: Totowa, NJ, 2004; pp 41−62. (d) Shoemaker, R. H. The NCI60 Human Tumour Cell Line Anticancer Drug Screen. *Nat. Rev. Cancer* **2006**, *6*, 813−823.
(27) (a) Plowman, J.; Dykes, D. J.; Hollingshead, M.; Simpson-Herren, L.; Alley, M. C.; Human Tumor Xenograft Models in NCI Drug Development. In *Anticancer Drug Development Guide: Preclinical Screening, Clinical Trials, and Approval*; Teicher, B., Ed.; Humana Press: Totowa, NJ, 1997; pp 101−125. (b) Hollingshead, M. G.; Alley, M. C.; Camalier, R. F.; Abbott, B. J.; Mayo, J. G.; Malspeis, L.; Grever, M. R. In vivo Cultivation of Tumor Cells in Hollow Fibers. *Life Sci.* **1995**, *57*, 131−141.
(28) Paull, K. D.; Lin, C. M.; Malspeis, L.; Hammel, E. Identification of Novel Antimitotic Agents Acting at the Tubulin Level by Computer-Assisted Evaluation of Differential Cytotoxicity Data. *Cancer Res.* **1992**, *52*, 3892−3900.
(29) Palaska, E.; Aytemir, V.; Uzbay, I. T.; Erol, D. Synthesis and Antidepressant Activities of Some 3,5-Diphenyl-2-pyrazolines. *Eur. J. Med. Chem.* **2001**, *36*, 539−543.
(30) Özdemir, A.; Turan-Zitouni, G.; Kaplancikli, Z. A.; Revial, G.; Güven, K. Synthesis and Antimicrobial Activity of 1-(4-Aryl-2-thiazolyl)-3-(2-thienyl)-5-aryl-2-pyrazoline Derivatives. *Eur. J. Med. Chem.* **2007**, *42*, 403−409.
(31) *CrysAlis PRO*, version 1.171.35.4; Agilent Technologies Ltd. (Oxford Diffraction): Yarnton, U.K., 2009.
(32) Sheldrick, G. M. A Short History of SHELX. *Acta Crystallogr.* **2008**, *A64*, 112−122.
(33) Farrugia, L. J. *ORTEP*-3 for Windows—A Version of ORTEP-III with a Graphical User Interface (GUI). *J. Appl. Crystallogr.* **1997**, *30*, 565.
(34) *CrysAlis PRO*, version 1.171.33.41c; Agilent Technologies Ltd. (Oxford Diffraction): Yarnton, U.K., 2009.